World Academy of Science, Engineering and Technology
International Journal of Biomedical and Biological Engineering
Vol:14, No:12, 2020

Optimization of Mechanical Properties of Alginate Hydrogel for 3D Bio-Printing Self-Standing Scaffold Architecture for Tissue Engineering Applications

Ibtisam A. Abbas Al-Darkazly

Open Science Index, Biomedical and Biological Engineering Vol:14, No:12, 2020 publications.waset.org/10011703.pdf

***Abstract*—**In this study, the mechanical properties of alginate hydrogel material for self-standing 3D scaffold architecture with proper shape fidelity are investigated. In-lab built 3D bio-printer extrusion-based technology is utilized to fabricate 3D alginate scaffold constructs. The pressure, needle speed and stage speed are varied using a computer-controlled system. The experimental result indicates that the concentration of alginate solution, calcium chloride ($CaCl_2$) cross-linking concentration and cross-linking ratios lead to the formation of alginate hydrogel with various gelation states. Besides, the gelling conditions, such as cross-linking reaction time and temperature also have a significant effect on the mechanical properties of alginate hydrogel. Various experimental tests such as the material gelation, the material spreading and the printability test for filament collapse as well as the swelling test were conducted to evaluate the fabricated 3D scaffold constructs. The result indicates that the fabricated 3D scaffold from composition of 3.5% wt alginate solution, that is prepared in DI water and 1% wt $CaCl_2$ solution with cross-linking ratios of 7:3 show good printability and sustain good shape fidelity for more than 20 days, compared to alginate hydrogel that is prepared in a phosphate buffered saline (PBS). The fabricated self-standing 3D scaffold constructs measured 30 mm × 30 mm and consisted of 4 layers (n = 4) show good pore geometry and clear grid structure after printing. In addition, the percentage change of swelling degree exhibits high swelling capability with respect to time. The swelling test shows that the geometry of 3D alginate-scaffold construct and of the macro-pore are rarely changed, which indicates the capability of holding the shape fidelity during the incubation period. This study demonstrated that the mechanical and physical properties of alginate hydrogel could be tuned for a 3D bio-printing extrusion-based system to fabricate self-standing 3D scaffold soft structures. This 3D bioengineered scaffold provides a natural microenvironment present in the extracellular matrix of the tissue, which could be seeded with the biological cells to generate the desired 3D live tissue model for *in vitro* and *in vivo* tissue engineering applications.

***Keywords*—**Biomaterial, calcium chloride, 3D bio-printing, extrusion, scaffold, sodium alginate, tissue engineering.

I. Introduction

CURRENTLY, 3D bio-printing technology to fabricate complex 3D living biological models on a bioengineered scaffold system has shown significant potential in the field of tissue engineering (TE) and regenerative medicine. 3D bioengineered scaffolds are made-up from biocompatible and printable materials, either integrated with live biological cells or seeded with the desired cells [1], to enable fabrication of patient-specific tissue models, living replacement tissue and devices, and for education purposes to improve patients' lives [2]. 3D bio-printing technology enables a geometrically precise 3D scaffold to be fabricated easily, providing physical support to the freshly developed tissue and to act as templates for living cells to grow and interaction, either *in vitro* or in *vivo* [3], [4]. The 3D bioengineered scaffold is an enabling technique, that can be utilized to reproduce or repair of cartilage tissue [2], [5], bone tissue [6], [5], skin tissue [7], cardiovascular tissue [8], and many more living tissue models [9]. There are two factors that form the use of scaffold: (1) the fabrication technique, and (2) the choice of biomaterial to construct a scaffold. The techniques of extrusion, inkjet, and laser technology are the main methods used in bioprinting [10], with extrusion based bioprinting being the most commonly used. The extrusion 3D bio-printing system can print various materials and compositions, including low viscosity and high viscosity biomaterials, such as complex polymers [11], to construct an appropriate 3D scaffold.

A. Biomaterial

Polymers of natural and synthetic source can be used as bioink materials. Polymers of natural origin such as alginate, gelatin, collagen, chitosan, hyaluronic acid, fibrin, etc., are the most prominent bioink materials. This is because, compared to synthetic polymers [1], they have higher biocompatibility, and biodegradability properties, and can provide the natural extracellular matrix (ECM) for cells to grow, and support cell viability. In particular, natural hydrogel-based biomaterials are consisting of cross-linked polymer chains with good mechanical characteristics and high affinity for water-swollen, which could provide a proper environment for the cell to generate new tissue or repair existing tissue [12]-[14]. Among the most widely used natural polymer hydrogels is alginate hydrogel. Alginate hydrogel is mainly attractive in wound healing, drug delivery systems and for the design and fabrication of 3D cell culture scaffolds to study a range of underlying biological mechanisms of human diseases in the lab to create better targeted drug therapeutics [15].

B. Alginate Structure

Alginate is an anionic polysaccharide and highly biocompatible material whose physical properties can be tailored to use in various TE applications. In addition, alginate hydrogels are characterized by a wide pore size distribution

Ibtisam A.Abbas Al-Darkazly, PhD, is with the School of food and Advanced Technology, Massey University, Auckland 0632, New Zealand (e-mail: aibtisam@hotmail.com).

Open Science Index, Biomedical and Biological Engineering Vol:14, No:12, 2020 publications.waset.org/10011703.pdf

(5-200 mm), which facilitates the diffusion of large molecules in and out of the gel [16]. Alginate is a copolymer consisting of two organic acid monomers, β-D-mannuronic acid (M) and α-L-guluronic acid (G) monomer units [12], (Figs. 1 (a) and (b)). Alginate is a negatively charged linear (M and G) acid blocks, which are polar solute soluble into water. The ratios of these acid blocks, as well as the choice of cross-linker and gelling conditions have a significant effect on its physical and mechanical properties. Alginate consists of chain of units that are ionically cross-linked by specific ions such as calcium (Ca^{2+}) to form a network of chains, resulting in a hydrogel gelation. This cross-linking is achieved by ionic interaction between (Ca^{2+}) ions and the carboxyl groups of the guluronic acid (G) residues of two neighboring alginate chains, forming a three-dimensional network model, (Fig. 2), resulting in a gel structure [15], [17]-[19]. Typically, calcium chloride ($CaCl_2$) is the most ionic cross-linker, leading to rapid gelation due to its high solubility in aqueous solutions [15]. Chemically cross-linked alginate hydrogel is normally used to ensure the mechanical stability of the 3D scaffold constructs. Alginate concentration, cross-linker concentration as well as gelling conditions plays an important role in the fabrication of 3D scaffold constructs [15]. However, maintaining the shape fidelity of the self-standing 3D scaffold constructs, using alginate hydrogel is still challenging. The mechanical properties of alginate hydrogel can be tuned through varying the cross-linking ratio (alginate:cross-linker) alone, with stiffness increasing, and hence, viscosity, with increases in the available cross-linker. Generally, low viscosity hydrogel is incapable of sustaining the shape fidelity after scaffold fabrication. On the other hand, high viscosity hydrogel could mechanically support the scaffold geometry [20], but it is not desirable for cell viability and proliferation [21]. Besides, high viscosity hydrogel needs high pressure to dispense the bioink material out of the nozzle, and hence, the encapsulated cell experiences shear stress causing cell damage. However, alginate hydrogel properties, including mechanical properties and printability, could be tailored during the fabrication process to meet specific needs, such as size, shape, porosity, and shape fidelity. These requirements may vary depending on the target tissue. As a soft structure, significant improvements in alginate hydrogel physical and mechanical properties are still needed, in terms of ability to maintain stand-alone 3D soft structures and to control the 3D microstructure, when they are printed, so that they do not deform or collapse.

In this work, the alginate concentration, $CaCl_2$ concentration as well as gelling conditions, including hardening time and temperature, are investigated, and are optimized for self-supporting 3D scaffold architecture with proper shape fidelity. The properties of alginate hydrogel can be tuned for optimal mechanical properties and printability, for stand-alone 3D soft structures to generate the desired 3D tissue model for *in vitro* tissue engineering applications.

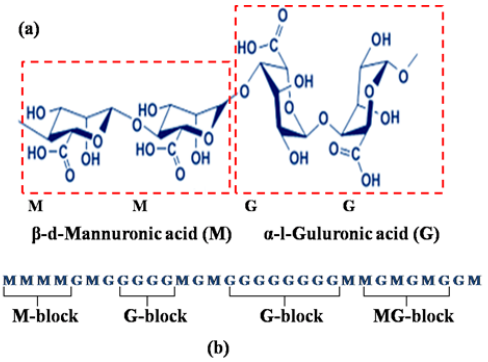

Fig. 1 (a) The chemical structures of β-d-mannuronic acid (M) and α-l-guluronic acid (G), (b) their distribution in the polymeric chain. The featured model is a sketch based on the model from [15]

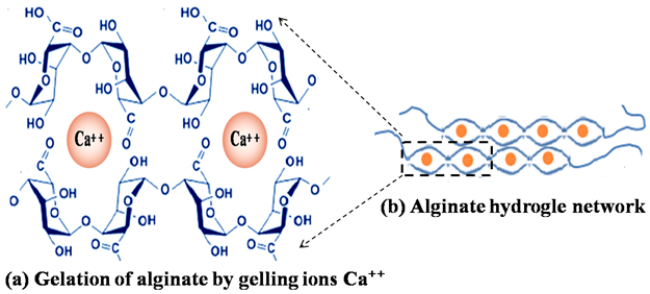

Fig. 2. Formation of an intermolecular network of alginate hydrogel by coordination of Ca^{2+} cations between adjacent alginate chains. The featured model is a sketch based on the model from [19]

II. Materials and Methods

A. Materials

Sodium alginate powder (A0682), calcium chloride ($CaCl_2$) powder (C4901), PBS (P4417), deionized water (DI) (38796), syringe needles (18- Z118044, 25-Z192414, 27-Z192376, and 30-Z192341gauge) were purchased from Sigma Aldrich. Distilled water was used for all experiments.

B. Extrusion-Based 3D Bio-Printing System

A three-axis in-lab built 3D bio-printer, equipped with syringe pump extruder (KD Scientific) system, was developed to print various materials, including biopolymers, low viscosity and high viscosity hydrogels, and fluids, by controlling the pressure, the printing speeds and utilizing standard syringe sizes with an appropriate needle. The developed 3D printer utilized a stepper motor to drive the syringe extruder. The 3D bio-printing system is supported by a computer controlled system for controlling needle speed, stage speed, and the "start/end" of the printer system to enable bioprinting of highly complex 3D scaffold constructs. The CAD model was created using SolidWorks software (Dassault Systems, 3D design software) and converted to an STL file. Fig. 3 shows the experimental set-up for the extrusion-based 3D bio-printing system and process.

C. Preparation of Alginate Hydrogel

The preparation of alginate hydrogel was performed according to the protocol described in [22], [23], and was

Open Science Index, Biomedical and Biological Engineering Vol:14, No:12, 2020 publications.waset.org/10011703.pdf

slightly modified for achieving an optimum alginate hydrogel result. At first, different concentrations of alginate solutions such as 2, 2.5, 3, 3.5, 4, 4.5 and 5% wt were prepared by dissolving the alginate powder in either DI water or in a PBS. The two alginate solutions were then stirred and sterilized using a magnetic hot plate, by autoclaving at 60 °C for 1 hour, and at room temperature for 1 hour to achieve a homogeneous composite. Both solutions were then stored in 4 °C fridge and used as sterile solutions for one to four weeks. Similarly, different concentrations of $CaCl_2$ solutions such as 0.5, 1, 2, 3, 4, and 5 % wt for cross-linking the alginate were also prepared by dissolving $CaCl_2$ powder into DI water. To form alginate hydrogels, the two solutions were pre-cross-linked by mixing the alginate solutions (in either DI water or in a PBS) with $CaCl_2$ solution at varying volumetric ratios (v/v) (25:9, 7:3, 2:1 and 4:3). The relative concentrations of alginate solutions and $CaCl_2$ solutions were both varied. Consequently, alginate hydrogels could crosslink at 40 °C for 30 minutes, and for 1 hour at room temperature prior to print. Alginate concentration, $CaCl_2$ concentration and gelling conditions (hardening time and temperature) were optimized for optimal printability. The variation of alginate concentration, $CaCl_2$ cross-linking concentration and the cross-linking ratios, as well as gelling conditions such as cross-linking reaction time and temperature, lead to the formation of alginate hydrogel with various gelation status. The prepared compositions of the studied formulation are shown in Table I. The optimal composition of the alginate hydrogel for the two alginate solutions (in either DI water or in a PBS) was found to include 3.5% wt alginate and 1% wt $CaCl_2$ at the determined optimum cross-linking ratios. The optimal composition was then used throughout the following experiments to evaluate the alginate hydrogel for printability test and structural characteristic of the fabricated 3D scaffold constructs.

D. Fabrication of 3D Scaffold Constructs

To fabricate the 3D scaffold constructs, alginate hydrogel was loaded into a sterilized 50 mL syringe in the printer (here containing blue-dyed alginate), and was subsequently deposited through a 25-gauge syringe needle layer-by-layer on a stationary print plate for printing at room temperature.

The fabricated scaffold was then incubated in 4% calcium chloride solution for 10 seconds cross-linking. After incubation, the fabricated scaffold was then rinsed briefly in DI water.

Various concentrations of alginate solutions and ionic cross-linker solutions were used to evaluate the material gelation state and the printability of the generated alginate hydrogels. The process parameters, such as printing temperature, extrusion speed, and pressure were optimized in this study. Alginate hydrogel flow rate and width of the filament were then optimized by controlling the printing speed, needle gauge, print distance (the distance from the needle tip to build plane) and dispensing pressure. The pressure is optimized by considering the continuity and stability of the alginate hydrogel extruded from the needle, and by varying other parameters such as the needle gauge. The optimized parameters of 3D bio-printing system for alginate hydrogels material were obtained as temperature 25 °C, pressure 150 kPa, and speed 100 mm/min. However, using less pressure could not exceed the surface tension of the material with the needle, and ultimately, will not deposit continuous filament.

TABLE I
COMPOSITION OF THE ALGINATE HYDROGELS

Ratios (v/v) 25:9, 7:3, 2:1, 4:3								
Formulation Concentrations % wt							DI (ml)	PBS (ml)
Alginate	2	2	2	2	2	2	100	100
$CaCl_2$	0.5	1	2	3	4	5	100	-
Formulation								
Alginate	2.5	2.5	2.5	2.5	2.5	2.5	100	100
$CaCl_2$	0.5	1	2	3	4	5	100	-
Formulation								
Alginate	3	3	3	3	3	3	100	100
$CaCl_2$	0.5	1	2	3	4	5	100	-
Formulation								
Alginate	3.5	3.5	3.5	3.5	3.5	3.5	100	100
$CaCl_2$	0.5	1	2	3	4	5	100	-
Formulation								
Alginate	4	4	4	4	4	4	100	100
$CaCl_2$	0.5	1	2	3	4	5	100	-
Formulation								
Alginate	4.5	4.5	4.5	4.5	4.5	4.5	100	100
$CaCl_2$	0.5	1	2	3	4	5	100	-
Formulation								
Alginate	5	5	5	5	5	5	100	100
$CaCl_2$	0.5	1	2	3	4	5	100	-

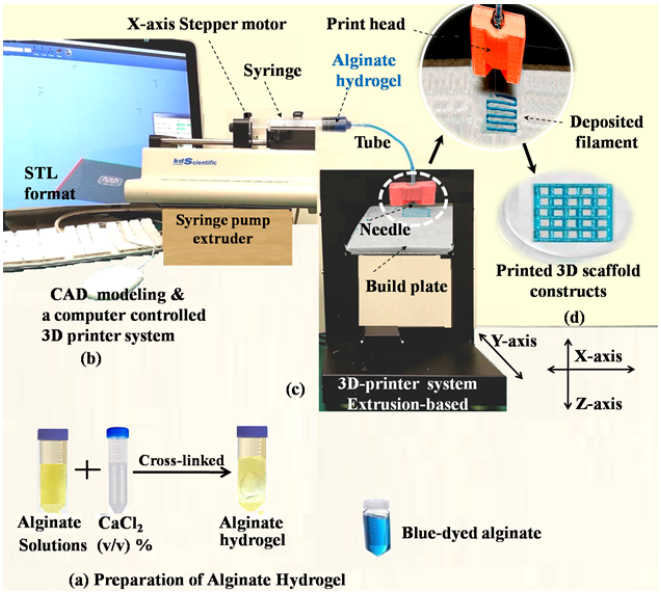

Fig. 3 Experimental set-up for 3D bioprinting system, and, 3D alginate-scaffold fabrication process

The printability and shape fidelity of different compositions of alginate hydrogel were investigated at a variety of cross-linking ratios (v/v) of 25:9, 7:3, 2:1 and 4:3 by using alginate solutions that were prepared in either DI water or in a PBS with $CaCl_2$ cross-linking solution. Various experimental tests

Open Science Index, Biomedical and Biological Engineering Vol:14, No:12, 2020 publications.waset.org/10011703.pdf

such as material gelation, material spreading and the printability test for filament collapse as well as a swelling test were then conducted to evaluate the generated alginate hydrogel and the fabricated 3D scaffold constructs.

E. Material Gelation for Printability Test

Material gelation was determined by examining the free-fall suspension of alginate hydrogel at the specified parameters such as temperature, pressure, and speed of the 3D bio-printer system. Various compositions of alginate solutions (either DI water or in a PBS), and $CaCl_2$ ionic cross-linker solutions at a variety of cross-linking ratios of (v/v) (25:9, 7:3, 2:1 and 4:3) were used in this test. If the material shows droplet flow pattern, the material is classified as under-gelation state (low viscosity), while irregular filament indicates over-gelation state (high viscosity). The only the straight line filament is characterized as proper-gelation. The findings will be provided in the results section.

F. Material Spreading and Printability Test

The rate of material spreading (percentage of diffusion rate (Df_r)) and printability (Pr) for the fabricated 3D alginate-scaffold constructs for each composition at a variety of cross linking ratios (v/v) of 25:9, 7:3, 2:1 and 4:3, were performed and determined respectively, using (1) and (2) as in [24], [25]:

$$Df_{r=\frac{A_t-A_a}{A_t}\times 100\%} \quad (1)$$

$$P_r = \frac{L^2}{16A_a} \quad (2)$$

where, A_t and A_a are theoretical and actual area of pore respectively, while L is the perimeter of the actual pore. The percentage of the diffusion rate and the printability of a pore are dependent on many factors such as pore size, needle gauge, dispensing pressure, temperature, printing speed and print distance. In general, the diffusion rate is decreasing while the printability is increasing, with increasing the pore size for each composition of material. However, the lower diffusion rates and the printability in the range of about 0.76-1.03 are desirable to allow the fabrication of proper self-standing 3D hydrogel structures and proper pore size with high precision [24]. The fabricated self-standing 3D scaffold structures, measured 30 mm × 30 mm and consisted of 4 layers (n = 4). Each pore of the fabricated 3D bio-printed structures is almost square in shape.

G. Swelling Study

The swelling test was performed using the protocol described in [4], [26], [27]. In the first step, after printing and the consequent cross-linking processes, the fabricated self-standing 3D scaffold was placed on a piece of filter paper and dried at room temperature until stable weight was achieved. The weight of the scaffold was then measured and considered as dry weight. The scaffold was then placed in a petri dish and around 50 ml distilled water was added to cover the scaffold and was subsequently incubated for different time periods. The scaffold was then tested for swelling behavior at room temperature. The percentage of swelling was determined by measuring the change of the weight of the sample as a function of incubation time using (3) [4], [26]:

$$\%\ \text{of swelling} = \frac{W_w - W_d}{W_d} \text{ X } 100 \quad (3)$$

where, W_d is the dry weight and W_w is the wet weight.

H. Statistical Analysis and Data Illustration

Statistical analysis was performed using Graph Pad Prism 7.0 Software. Quantitative analysis was examined using two-way ANOVA test followed by Tukey's Multiple Comparison Test. A minimum of five independent experiments (n = 5) were utilized for the statistical analysis. Results are expressed as mean ± standard deviation.

III. Results

A. Material Gelation Test Results

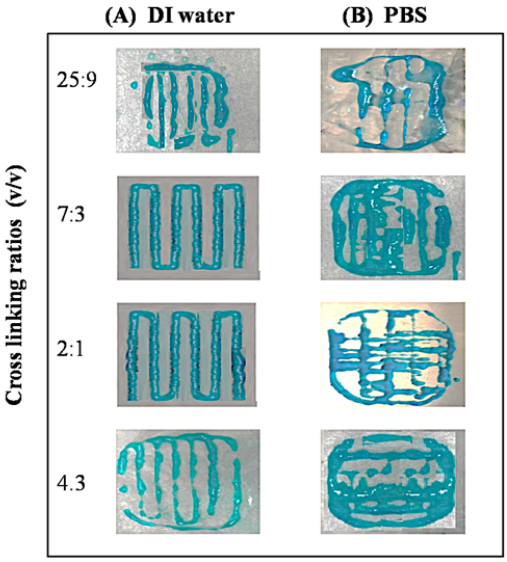

Fig. 4 Evaluation material gelation status of alginate hydrogel for alginate solutions that were prepared in DI water (A) and in a PBS (B) with $CaCl_2$ solution at a variety of cross linking ratios (v/v) of (25:9, 7:3, 2:1 and 4:3). Images of the design pattern used to investigate material gelation status of the prepared alginate hydrogel for the two alginate solutions

Fig. 4 shows the material gelation status of the prepared alginate hydrogels. Various concentrations of alginate and ionic cross-linker solutions were used to evaluate the material gelation status. The material gelation test indicates that the alginate hydrogel gets from under gelation state (low viscosity) (25:9) or over-gelation state (high viscosity) (4:3) to gelation state (2:1) and proper gelation state (an appropriate viscosity) (7:3) when relative increases in cross-linking ratios. However, the alginate hydrogel with composition of 3.5% wt that was prepared in DI water and 1% wt $CaCl_2$ solution, with cross-linking ratios of 7:3 (Fig. 4 (A)), generates almost a straight filament at various distances, which indicates the optimum alginate hydrogel for self-standing 3D scaffold

Open Science Index, Biomedical and Biological Engineering Vol:14, No:12, 2020 publications.waset.org/10011703.pdf

constructs. On the other hand, various compositions of alginate that were prepared in a PBS and $CaCl_2$ solution with various cross-linking ratios, including composition of 3.5% wt and 1% wt $CaCl_2$ solution and cross-linking ratios of 25:9, 7:3, 2.1 and 4:3 respectively, did not make proper gelation (Fig. 4 (B)). The material generates irregular and curvy filament, and almost collapsed, which could disrupt the printability and shape fidelity of the alginate-scaffold constructs. The statistical analysis confirming the results from five independent experiments is shown in Fig. 5, which is quantified as a percentage of the material gelation status.

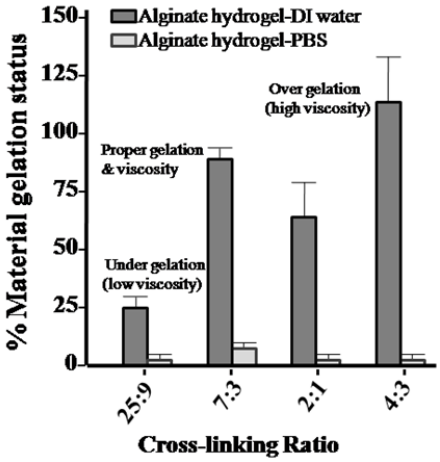

Fig. 5 Statistical analysis of material gelation status of alginate hydrogels from five independent experiments. (Two ways ANOVA Kruskal-Wallis Test followed by Tukey's Multiple Comparison Test). Error bars denote standard deviation, (n = 5)

B. Material Spreading and Printability Test Results

Fig. 6 shows the material spreading and printability test of the fabricated 3D alginate-scaffold constructs. The fabricated 3D scaffold for each composition at a variety of cross linking ratios (v/v) of 25:9, 7:3, 2:1 and 4:3 consisted of 4 layers (n = 4), follows 0^0-90^0 pattern as shown in Fig. 6 (a). To determine the effect of filament separation and pore closing for the printed 3D scaffold constructs, the actual area (Aa) and the perimeter (L) of each pore of the printed scaffold were measured, and the percentage of diffusion rate (*Dfr*) and printability (*Pr)* were calculated using (1) and (2).

The images of a single filament and of fabricated 3D alginate scaffolds were taken with canon power shot A470 high resolution digital camera for image acquisition. Pore size, thread diameter and filament widths were measured using Nikon confocal microscope for each of this test. The experimental measurements were carried out several times and the plotted values were confirmed from five repeated trials for each alginate composition.

The printed 3D scaffold constructs for the optimal composition of 3.5% wt alginate solution (in DI water) with 1% wt $CaCl_2$ solution at cross linking ratios of 7:3, and 2:1 (Figs. 6 (c) and (d)) show good pore geometry and less material spreading (minimum diffusion rate) than other cross-linking ratios as shown in Fig. 7 (percentage of diffusion rate (*Dfr*) graph). However, the fabricated scaffold in Fig. 6 (c) shows an almost square shape of the pore with high precision compared to other alginate compositions. Alginate compositions at cross linking ratios (v/v) of 25:9 and 4:3, (scaffold constructs are not shown). The statistical analysis of material spreading test confirming the results from five independent experiments is shown in Fig. 8.

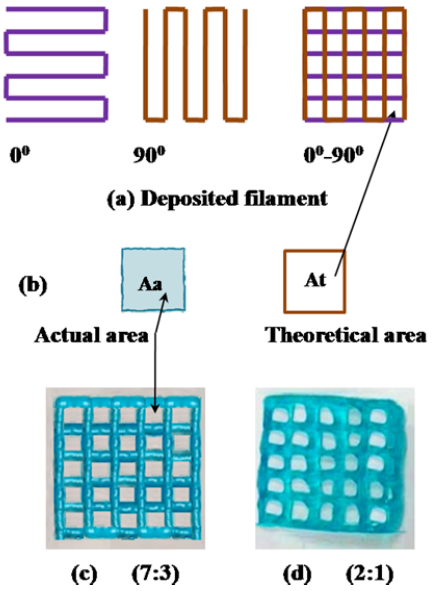

Fig. 6 Material spreading and printability test for the fabricated 3Dalginate-scaffold. (a) Filament deposited from 0^0, 90^0 and 0^0-90^0. (b) Theoretical and actual area of the pore. (c) Self-standing 3D alginate-scaffold constructs from composition of 3.5% wt alginate solution (in DI water) and 1% wt $CaCl_2$ solution, with cross-linking ratios of 7:3 and 2:1

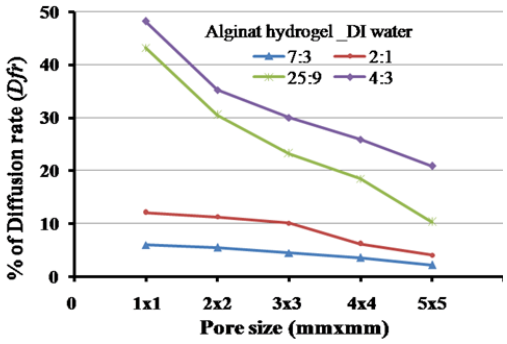

Fig. 7 The percentage of diffusion rate (*Dfr*) for the fabricated 3D scaffolds for each composition at a variety of cross-linking ratios (v/v) of 25:9, 7:3, 2:1 and 4:3

The range of printability in Fig. 9 for the optimal composition of 3.5% wt alginate (in DI water) with 1% wt $CaCl_2$ at cross-linking ratios of 7:3 and 2:1 is about 0.81-1.02 and 0.83-1.09 respectively, which are desirable. The statistical analysis of printability test confirming the results from five independent experiments is shown in Fig. 10. However, the geometry of the pore for the 3D scaffold that formed from the alginate solution with composition of 3.5% wt, that was prepared in DI water and 1% wt $CaCl_2$ solution, with cross-

Open Science Index, Biomedical and Biological Engineering Vol:14, No:12, 2020 publications.waset.org/10011703.pdf

linking ratios of 2:1 is not uniform (Fig. 6 (d)). This could be due to the fact that the material may not reach proper gelation state. The various compositions of alginate solutions that were prepared in a PBS with various cross-linking ratios did not make good pore geometry (shape and data are not shown).

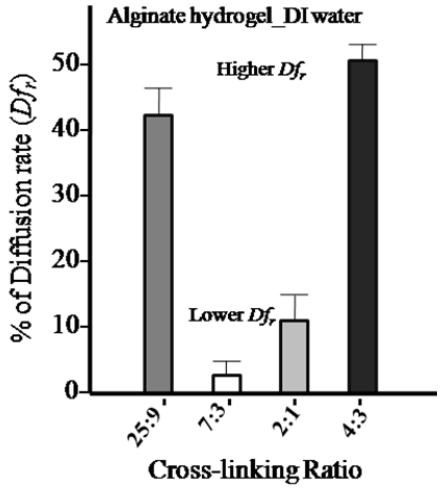

Fig. 8 Statistical analysis of the percentage of diffusion rate (*Dfr*) of the fabricated self-standing 3D alginate-scaffold from five independent experiments. (One way ANOVA Kruskal-Wallis Test followed by Tukey's Multiple Comparison Test). Error bars denote standard deviation, (n = 5)

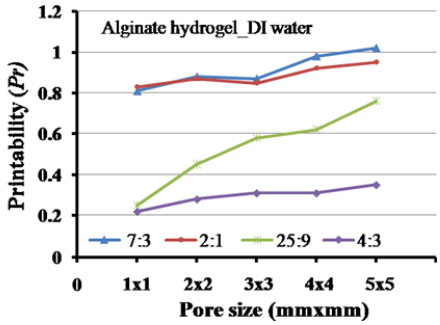

Fig. 9 Printability (*Pr)* test for different material compositions

C. Structural Characteristics of the 3D Scaffold Constructs

The structural characteristics and long-term stability of the optimal alginate-scaffold constructs (3.5% wt in DI water and 1% wt $CaCl_2$, with cross-linking ratios of 7:3) after chemical cross-linking by $CaCl_2$ solution were investigated in this work. The self-standing 3D scaffold constructs measured 30 mm × 30 mm and consisted of 4 layers (n = 4). The printed 3D scaffold constructs show clear grid structure after printing as shown in Fig. 11. Each pore of the fabricated 3D alginate-scaffold is almost square in shape. The pore size (A), thread diameter (B) and maximum pore distance (filament width) (C) of the 3D scaffold constructs maintained the integrity with clear grid structure for more than 10 days (Figs. 11 (a) and (b)). Indeed, the grid structure sustained stable for more than 20 days ((Fig. 11 (c)) as long as it located to the bottom of the Petri dish rather than floating in the medium.

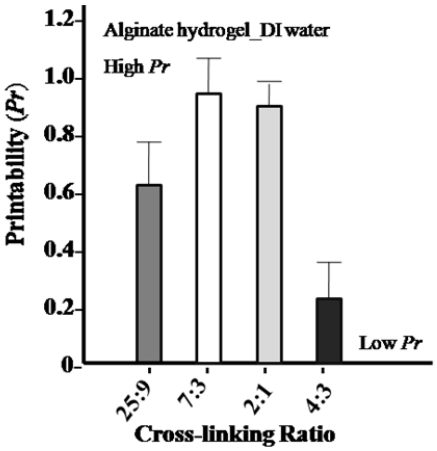

Fig. 10 Statistical analysis of the printability (*Pr*) test of the fabricated self-standing 3D alginate-scaffold from five independent experiments. (One way ANOVA Kruskal-Wallis Test followed by Tukey's Multiple Comparison Test). Error bars denote standard deviation, (n = 5)

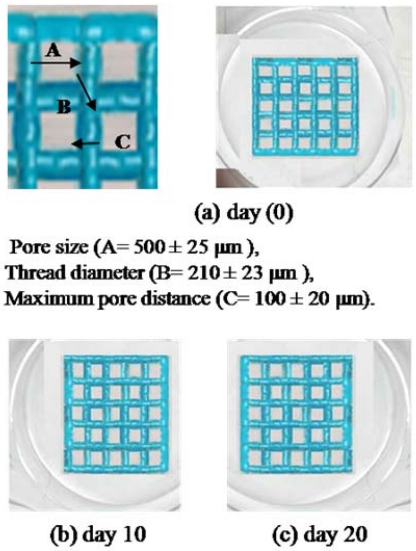

Fig. 11 Self-standing 3D alginate-scaffold stability over time. (a) The scaffold configuration after printing at day 0. (b) The scaffold integrity at day 10 and (c) at day 20. Scale: 1 mm

D. Swelling Test Result

The geometry of the 3D alginate-scaffold and of the macro-pore is seldom changed during the incubation period as shown in Fig. 12, which indicates its capability to hold shape fidelity during the incubation period. Fig. 13 shows the percentage change of swelling degree as a function of time for the fabricated 3D alginate-scaffold. As can be seen in the swelling graph the percentage change of swelling degree exhibits high swelling capability with respect to time. The 3D alginate-scaffold reached its equilibrium state of swelling at about 10 day, which completed full expansion of the hydrogel network. The percentage swelling of the scaffold increased about 250% times over dry sample, when it reached equilibrium in 10 days. The statistical analysis confirming the results from five independent experiments is shown in Fig. 14 which is

Open Science Index, Biomedical and Biological Engineering Vol:14, No:12, 2020 publications.waset.org/10011703.pdf

quantified as the percentage change of swelling degree as a function of time.

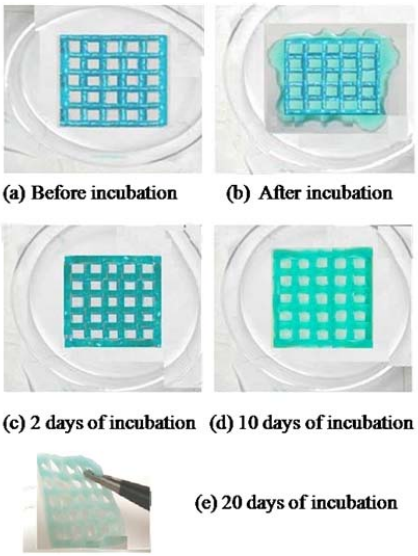

Fig. 12 Swelling test for the fabricated self-standing 3D alginate-scaffold

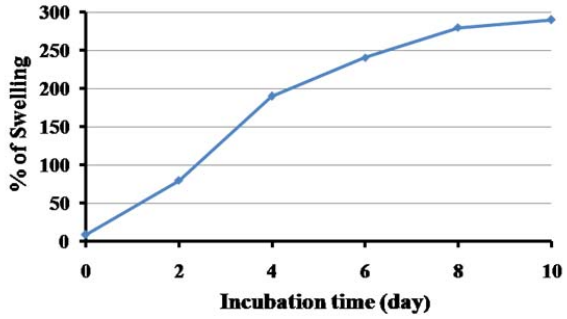

Fig. 13 Percentage of swelling of the self-standing 3D alginate-scaffold as a function of incubation time (day)

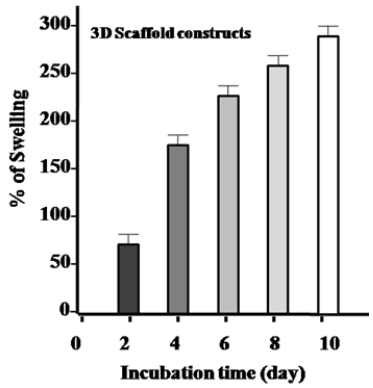

Fig. 14 Statistical analysis of swelling degree of the fabricated self-standing 3D alginate-scaffold as a function of swelling time from five independent experiments. (One way ANOVA Kruskal-Wallis Test followed by Tukey's Multiple Comparison Test). Error bars denote standard deviation, n = 5)

IV. Discussion

In this study, the mechanical and physical properties of alginate hydrogel material were optimized for 3D bio-printing extrusion-based techniques to fabricate self-standing 3D scaffold constructs. Various concentrations of alginate solutions that were prepared by dissolving the alginate powder in either DI water or in a PBS were used in this study. Both alginate solutions were then pre-cross-linked by using $CaCl_2$ solution at varying volumetric ratios (v/v) of (25:9, 7:3, 2:1 and 4:3) to generate alginate hydrogel. Alginate concentration, $CaCl_2$ concentration and cross-linking ratios as well as gelling conditions such as gelation rate, hardening time and temperature were optimized in this study. The result reveals that the composition of alginate (PBS versus DI water), cross-linking ratio and gelling conditions influence the printability and shape fidelity of the generated alginate hydrogel. Several characterization tests such as the material gelation, the material spreading and the printability test for filament collapse, and the swelling test were then conducted to evaluate the printability and shape fidelity of each composition and of the fabricated 3D alginate-scaffold constructs. The experimental results show that the composition of 3.5% wt alginate that was prepared in DI water and 1% wt $CaCl_2$ solution, with cross-linking ratios of 7:3 (Fig. 4 (A)), generates an optimum alginate hydrogel. The material gelation status of this composition compares well to that obtained from other cross-linking ratios and from alginate solution that were prepared in a PBS of this study, as well as [23]. It generates an almost straight filament at various distances with the printability in the range of about 0.81-1.02 (Fig. 9). As previously mentioned (see Section II *F* Material Spreading and Printability Test), lower spreading ratios and the printability in the range of about 0.76-1.03 are desirable to allow fabrication of high precision 3D scaffold structures with proper pore size [24]. However, at high cross-linking ratios of 25:9, the alginate hydrogel became under cross-linked, and its viscosity was so low, hence, unprintable. Also, at low cross-linking ratios of 4:3, the alginate hydrogel became over cross-linked; hence, the viscosity of alginate hydrogel was so high and made it very difficult to go over a designed 3D printing pattern, as shown in Fig. 4 (A). The fabricated self-standing 3D scaffold measured 30 mm × 30 mm and consisted of 4 layers (n = 4) and shows clear grid structure after printing. The printed self-standing 3D scaffold for the optimal composition of alginate hydrogel (Fig. 6 (c)) shows good pore geometry and less material spreading than other alginate compositions ((*Dfr*) graph in Fig. 7). The pore size, thread diameter and filament width of the self-standing 3D scaffold maintained the integrity with clear grid structure for more than 20 days (Figs. 11 (a)-(c)). On the other hand, alginate hydrogel that was prepared in a PBS over DI water can considerably affect the mechanical properties of alginate hydrogel and hence, its printability. It was found that preparing alginate solution in PBS at a variety of cross-linking ratios (Fig. 4 (B)) generates irregular and curvy filament and was almost collapsed, which could disrupt the printability and shape fidelity of the 3D alginate-scaffold constructs. Studies [23], [28] demonstrated

Open Science Index, Biomedical and Biological Engineering Vol:14, No:12, 2020 publications.waset.org/10011703.pdf

that using PBS to prepare alginate hydrogel can considerably reduce its mechanical properties. This is due to the fact that alginate hydrogel undergoes disintegration in the presence of calcium chelators, such as phosphate. As phosphate rapidly binds to Ca^{2+} ions, the alginate hydrogel became under cross-linked which affects its material gelation status, and hence, its mechanical integrity. PBS is a water-based salt solution, containing sodium phosphate, sodium chloride and, in some formulations, it contains potassium chloride and potassium phosphate [29], which could disrupt the mechanical integrity of alginate hydrogel material. Furthermore, alginate hydrogel could also undergo disintegration in the presence of monovalent ions such as Na^{+} [28]. Thus, preparing alginate hydrogel in NaCl-free solutions could improve material gelation status and hence, its mechanical properties. However, one great advantage of ionically cross-linked alginate is that, it can be dissolved and degraded by release of the divalent ions (Ca^{2+} cations) that cross-linking the gel into the physiological surrounding media due to exchange reactions with monovalent cations such as sodium ions [15], and hence, could completely remove from the body.

The result also shows that the gelation rate and gelation temperature are important factors in controlling hydrogel regularity, stability, and its strength, and, hence, the mechanical properties of the 3D scaffold structures. A variety of conditions were tested, ranging from instantaneous cross-linking reaction to slow reaction time, with various gelation temperatures. It has been found that the cross-linking reaction time for 30 minutes at 40 °C, and for 1 hour at room temperature prior to print lead to formation of alginate hydrogel with great mechanical reliability. Slow gelation rate at an appropriate low gelation temperature generates more uniform structures with superior mechanical integrity [30]. This is due to the fact that, at low gelation temperatures, the reactivity of ionic cross-linkers Ca^{2+} is decreased, and hence, cross-linking reaction becomes slower. Consequently, the resultant cross-linked network structure has greater regularity and stability over time [31]. Besides, the mechanical properties of ionically cross-linked alginate hydrogels vary depending on the chemical structure of alginate. As previously described (see Section I *B*) alginate is a copolymer consisting of two organic acid monomers, M and G monomer units. The ratio of these acid blocks has a significant effect on the mechanical properties of alginate hydrogel. Hydrogel prepared from alginate with a high content of G residues exhibits higher stiffness than those with a low amount of G residues [32]. This is because G- monomers have a high-affinity interaction with Ca^{2+}, hence, contributed strongly in intermolecular cross-linking with divalent cations (Ca^{2+}) to form alginate hydrogel [15], [19] while M monomers form weak junctions with divalent Ca^{2+}cations [19], [32].

The percentage change of swelling degree test, as a function of time, for the fabricated self-standing 3D scaffold exhibits high swelling capability with respect to time (Fig. 13), while its geometry and the macro-pore are seldom changed, which indicates its capability to hold the shape fidelity during the incubation period at a constant room temperature. The swelling ability of the alginate hydrogel is attributed to the presence of hydrophilic functional groups (ionic carboxyl groups) on its backbone (Fig. 2). However, the swelling percentage of the alginate gels increases as the concentration of sodium alginate increases and Ca^{2+} concentration decreases, due to change of the ionic carboxyl groups' strength [28]. This is due to the fact that the functional (carboxyl) groups of alginate chain create complex structure with Ca^{2+} ions. The increases of sodium alginate concentration, and subsequent increases in sodium alginate chain, give more functional (carboxyl) groups that can accumulate around Ca^{2+} cross-linking agent, and hence, further layers of alginate chain can join the Ca^{2+} cations to obtain alginate hydrogel. On the other hand, increasing the concentrations of $CaCl_2$ makes the alginate hydrogel more viscous, which probably could enhance printability, and achieve good shape fidelity, but high viscosity hydrogel could reduce the swelling ability of the alginate hydrogel [4]. Also, high viscosity hydrogel requires high air pressure to deposit the filament, which could limit the use of the available bio-printer. Furthermore, encapsulated cell in a high viscosity bioink will impose too much shear stress during suspension and eventually will be damaged the cell [24]. However, the time-dependent higher percentage of swelling produces more porosity in the alginate scaffold constructs which leads more exchange of nutrient and waste element of encapsulated cells during the incubation period [24].

V. Conclusion and Future Perspectives

The present study aimed to investigate the mechanical and physical properties of biocompatible alginate hydrogel material for self-supporting 3D alginate scaffold constructs. It found that alginate concentration, $CaCl_2$ cross-linking concentration and cross-linking ratios, as well as gelling conditions such as cross-linking reaction time and temperature, lead to the formation of alginate hydrogel with variable gelation status, which have a significant effect on its mechanical properties and printability of the 3D alginate-scaffolds network. In conclusion, this work demonstrated that the mechanical and physical properties of alginate hydrogel can be tuned for a 3D bio-printing process extrusion-based system to fabricate self-supporting 3D alginate scaffold architecture with proper shape fidelity. *In vitro*, 3D-bioengineered scaffolds to generate live tissue models are a pleasing tool to mimic the native biological tissue and its processes to assess understanding on critical and unique disease states. In particular, 3D live tissue models are being increasingly utilized to study a range of underlying biological mechanisms of human diseases in the laboratory, in order to design better targeted drug therapeutics. For example, a 3D bio-printed tumor model with live cancer cells provides an *in vitro* tool for the development of anticancer therapeutics, which will be employed in the future.

References

[1] J. Gopinathan and I. Noh, "Recent trends in bioinks for 3D printing," *Biomater Res, BMC J.*, vol.22, no.11, April 2018.

Open Science Index, Biomedical and Biological Engineering Vol:14, No:12, 2020 publications.waset.org/10011703.pdf

DOI.org/10.1186/s40824-018-0122-1.

[2] J. H.Y. Chung, J. Kade, A. Jeiranikhameneh *et. al,* "A bioprinting printing approach to regenerate cartilage for microtia treatment," *Elsevier, Bioprinting, J*. vol.12, no. e0031 pp.1-11, Dec. 2018. DOI.org/10.1016/j.bprint.2018.e00031

[3] Z. Wu, X. Su, Y. Xu *et al*, "Bioprinting three-dimensional cell-laden tissue constructs with controllable degradation," *Sci.Rep*, vol,6, no. 24474, April 2016. DOI.org/10.1038/srep24474

[4] I. Noh, N. Kim, H. N. Tran, *et al,* "3D printable hyaluronic acid-based hydrogel for its potential application as a bioink in tissue engineering," *Biomater Res***,** vol.23, no.3, Feb. 2019. DOI.org/10.1186/s40824-018-0152-8

[5] T. Xu, K. W. Binder, M. Z. Albanna *et al*, "Hybrid printing of mechanically and biologically improved constructs for cartilage tissue engineering applications", *Biofabrication,* vol.5, no.015001, Mar. 2013. DOI: 10.1088/1758-5082/5/1/015001

[6] J. Jeong, J. H. Kim, J. H. Shim, *et al*, "Bioactive calcium phosphate materials and applications in bone regeneration," *Biomater Res,* vol.23, no.4, Jan. 2019. DOI.org/10.1186/s40824-018-0149-3

[7] V. Lee, G. Singh, J. P. Trasatti *et al.,* "Design and fabrication of human skin by three-dimensional bioprinting," *Tissue Eng. Part C*: *Methods,* vol.20, no.6, pp.473–484, Jun. 2013.DOI: 10.1089/ten.TEC.2013.0335

[8] Simbara, Pimenta, Carbonari *et al.,* "A review on fibrous scaffolds in cardiovascular tissue engineering," *Innov Biomed Technol Health Care (IBTHC*), vol.1, no.1, pp.14 – 28, May 2017

[9] S.V. Murphy and A. Atala, "3D bioprinting of tissues and organs," *Nat. Biotechnol J*., vol.32, pp.773–785, Aug.2014. DOI.org/10.1038/nbt.2958

[10] M. Varkey, D.O. Visscher, P.P.M.V. Zuijlen *et al.,* "Skin bioprinting: the future of burn wound reconstruction?", *Burn Trauma J*., vol.7, no.4, Feb.2019. DOI.org/10.1186/s41038-019-0142-7

[11] E. S. Bishop, S. Mostafa, M. Pakvasa *et al*., "3-D bioprinting technologies in tissue engineering and regenerative medicine: Current and future trends," *Genes & Dis*., *ScienceDirect J*., vol.4, no.4, pp.185-195, Dec.2017. DOI: 10.1016/j.gendis.2017.10.002

[12] M. Ahearne, "Introduction to cell–hydrogel mechanosensing," *Interface Focus royal society*, vol.4, no.20130038 April 2014. DOI.org/10.1098/rsfs.2013.0038

[13] V. H. P. Luna and O. G. Reynoso, "Encapsulation of Biological Agents in Hydrogels for Therapeutic Applications," *Gels,* vol.3, no.61 Sep. 2018. DOI:10.3390/gels4030061

[14] U. Jammalamadaka and K. Tappa, "Recent Advances in Biomaterials for 3D Printing and Tissue Engineering," *Funct Biomater J*., vol.1, no.9, Mar. 2018. DOI: 10.3390/jfb9010022

[15] K. Y. Lee. &, D. J. Mooney, "Alginate: properties and biomedical applications," *Prog Polym Sci,* vol.37, no.1, pp.106–126, Jan. 2012. DOI.org/10.1016/j.progpolymsci.2011.06.003

[16] L. Gasperini, J. F. Mano and R. L. Rris, "Natural polymers for the microencapsulation of cells," *R Soc Interface J.,* vol.11, no.20140817 Nov. 2014. DOI.org/10.1098/rsif.2014.0817

[17] N. E., C. L. Stabler, C. P. Simpson *et al*., "The role of the CaCI2-guluronic acid interaction on alginate encapsulated bTC3 cells," *Biomaterials J*., vol.25, no.13, pp.2603-2610, Jun 2004. DOI: 10.1016/j.biomaterials.2003.09.046

[18] D. Kühbeck, J. Mayr, M. Häring *et al*., "Evaluation of the nitroaldol reaction in the presence of metal ion-crosslinked alginates," *New J. Chm*., vol. 39, pp.2306-2315, Jan. 2015. DOI.org/10.1039/c4nj02178a

[19] T. Andersen, P. A. Emblem and M. Domish, "3D Cell Culture in Alginate Hydrogels," Microarrays J., vol.4, no.2, pp.133-161, Jun. 2015. DOI: 10.3390/microarrays4020133

[20] Y. He, F. F. Yang, H. M. Zhao et al., "Research on the printability of hydrogels in 3D bioprinting, Sci Rep, vol.6, no.29977, Jul. 2016. DOI: 10.1038/srep29977

[21] S. Khalil, W. Sun, "Bioprinting endothelial cells with alginate for 3D tissue constructs," *Biomech Eng J*., vol.131, no.11, Nov.2009. DOI: 10.1115/1.3128729

[22] Y. Kim, K. Kang, J. Jeong *et al*., "Three-dimensional (3D) printing of mouse primary hepatocytes to generate 3D hepatic structure," *Ann Surg Treat Res*, vol.92, no.2, Feb. 2017. DOI: 10.4174/astr.2017.92.2.67

[23] F. E. Freeman and D. J. Kelly, "Tuning Alginate Bioink Stiffness and Composition for Controlled Growth Factor Delivery and to Spatially Direct MSC Fate within Bioprinted Tissues," *Sci Rep,* vol.7, no.17042, Dec. 2017. DOI:10.1038/s41598-017-17286-1

[24] M. A. Habib and B. Khoda, "Development of clay based novel bio-ink for 3D bio-printing process," *Procced Manufactuer, Elsevier*, vol.26, pp.846-856, 2018.DOI.org/10.1016/j.promfg.2018.07.105

[25] L. Ouyang, R. Yao, Y. Zhao and W. Sun, Effect of bioink properties on printability and cell viability for 3D bioplotting of embryonic stem cells, *Biofabrication*, vol.8, no.3, Sep. 2016. DOI: 10.1088/1758-5090/8/3/035020

[26] N. Devi and T. K. Maji, "Preparation and Evaluation of Gelatin/Sodium Carboxymethyl Cellulose Polyelectrolyte Complex Microparticles for Controlled Delivery of Isoniazid," *PMCID*, vol.4, no.1412, Dec. 2009. DOI: 10.1208/s12249-009-9344-9

[27] R. Mahdavinia, Z. Rahmani, S. Karami and A. Pourjavadi, "Magnetic/pH-sensitive κ-carrageenan/sodium alginate hydrogel nanocomposite beads: preparation, swelling behavior, and drug delivery" *Biomater Sci Polym Ed,* vol.25, no.17, pp.1891-1906, Sep. 2014. DOI: 10.1080/09205063.2014.956166

[28] M. Matyash, F. Despang, C. Ikonomidou, and M. Gelinsky, "Swelling and mechanical properties of alginate hydrogels with respect to promotion of neural growth," *Tissue Eng. Part C: Methods,* vol.20, no.5, pp.401-411, May2014 DOI: 10.1089/ten.tec.2013.0252.

[29] Sigma Aldrich. (2020) (Online). Available: https://www.sigmaaldrich.com/new-zealand

[30] C. K. Kuo and P. X. Ma, "Ionically crosslinked alginate hydrogels as scaffolds for tissue engineering: part1structure, gelation rate and mechanical properties," *Biomaterials Elsevier*, vol.22, no.6, pp.511-521 Mar. 2001.DOI.ORG/10.1016/S0142-9612(00)00201-5

[31] A. D. Augst, H. J. Kong and D. J. Mooney, "Alginate hydrogels as biomaterials," *Macromolecular Biosci*, vol.6, no.8, pp.623–633, July 2006. DOI.org/10.1002/mabi.200600069

[32] J. Sun and H. Tan, "Alginate-Based Biomaterials for Regenerative Medicine Applications," *Materials*, vol.6, no.4, pp.1285-1309, Mar. 2013. DOI:10.3390/ma6041285